Pflugers Arch - Eur J Physiol (2009) 458:795–807
DOI 10.1007/s00424-009-0662-2

SIGNALING AND CELL PHYSIOLOGY

Inhibition of N and PQ calcium channels by calcium entry through L channels in chromaffin cells

Juliana M. Rosa · Luis Gandía · Antonio G. García

Received: 16 October 2008 / Revised: 9 February 2009 / Accepted: 1 March 2009 / Published online: 4 April 2009

Abstract Why adrenal chromaffin cells express various subtypes of voltage-dependent Ca^{2+} channels and whether a given channel is specialized to perform a specific function are puzzling and unanswered questions. In this study, we have used the L Ca^{2+} channel activator FPL64176 (FPL) to test the hypothesis that enhanced Ca^{2+} entry through this channel favors the inhibition of N and PQ channels in voltage-clamped bovine adrenal chromaffin cells. Using 2 mM Ca^{2+} as charge carrier and under the perforated-patch configuration (PPC) of the patch-clamp technique, FPL caused a paradoxical inhibition of the whole-cell inward Ca^{2+} current (I_{Ca}). Such inhibition turned on into an augmentation upon cell loading with EGTA-AM. Also, under the whole-cell configuration (WCC) of the patch-clamp technique, FPL decreased I_{Ca} in the absence of EGTA from the pipette solution and increased the current in its presence. Using 2 mM Ba^{2+} as charge carrier, FPL augmented the Ba^{2+} current under both recording conditions, WCC and PPC. FPL augmented the residual current remaining after blockade of N and PQ channels with ω-conotoxin MVIIC or by holding the membrane potential at −50 mV. The data support the view that Ca^{2+} entering the cell through the lesser inactivating L channels serves to modulate the more inactivating N and PQ channels. They also suggest a close colocalization of L and N/PQ Ca^{2+} channels. This kind of L channel specialization may be relevant to cell excitability, exocytosis, and cell survival mechanisms.

Keywords L calcium channel · N calcium channel · PQ calcium channel · Chromaffin cells · Calcium current · FPL64176

J. M. Rosa · L. Gandía · A. G. García (✉)
Instituto Teófilo Hernando, Facultad de Medicina,
Universidad Autónoma de Madrid,
Arzobispo Morcillo,
4. 28029 Madrid, Spain
e-mail: agg@uam.es

J. M. Rosa · L. Gandía · A. G. García
Departamento de Farmacología y Terapéutica,
Facultad de Medicina, Universidad Autónoma de Madrid,
Madrid, Spain

A. G. García
Servicio de Farmacología Clínica,
Hospital Universitario de la Princesa, Facultad de Medicina,
Universidad Autónoma de Madrid,
Madrid, Spain

Introduction

Bovine chromaffin cells express neuronal voltage-dependent Ca^{2+} channels of the subtypes L (α_{1D}, $Ca_v1.3$), N (α_{1B}, $Ca_v2.2$), and PQ (α_{1A}, $Ca_v2.1$) [22], having similar biophysical and pharmacological properties to those expressed by neurons [20, 23, 59]. Why these cells express L as well as non-L (N/PQ) Ca^{2+} channels is an intriguing question. There are reports suggesting different modulation of channel subtypes and different roles in controlling exocytosis, according to various experimental conditions and patterns of chromaffin cell stimulation. The following findings illustrate this point: (1) Ca^{2+} channel currents (I_{Ca}) are modulated by neurotransmitters in a voltage-dependent (N/PQ channels) or voltage-independent manner (L channels) [1, 18, 19, 30]; (2) depending on the experimental conditions, L channels may be preferentially coupled to exocytosis [40] or PQ channels may dominate the control of secretion [36]; (3) cell stimulation with action potentials (APs) produce a secretory response mostly controlled by PQ channels, while secretion stimulated with depolarizing pulses

is controlled by other channel subtypes [14]; (4) L channels are tightly coupled to endocytosis while N/PQ channels are more weakly coupled to endocytosis [60, 63]; (5) L channels are more resistant to voltage-dependent inactivation while N/PQ channels are more prone to such inactivation [31, 70]; and (6) L channels undergo Ca^{2+}-dependent inhibition at a rate slower than N/PQ channels [32].

The Ca^{2+}-dependent inactivation of Ca^{2+} channels was first suggested by Hagiwara and Nakajima [28], subsequently proven by Brehm and Eckert [9] and Tillotson [68] in mollusc neurons, and later on extended to various excitable cells [27]. It is interesting to note that not all Ca^{2+} channel subtypes are equally prone to Ca^{2+}-dependent inactivation. For instance, the cardiac and smooth muscle L channel is quickly inactivated upon depolarization [25, 37, 52] while the neuronal L channel inactivates more slowly [71]. Because the L channel inactivates more slowly in bovine chromaffin cells [32], it may be that Ca^{2+} entry through this channel could modulate N/PQ channels. In this study, we tested this hypothesis by measuring the whole-cell inward Ca^{2+} channels current (I_{Ca}) in voltage-clamped bovine adrenal chromaffin cells. We used the L channel activator FPL64176 (FPL) [44, 75] to enhance the I_{Ca} flowing through L channels to test its consequences on the inhibition of the I_{Ca} flowing through N and PQ channels. The results support the hypothesis implying the existence of a Ca^{2+}-mediated cross-talk between L and N/PQ Ca^{2+} channels.

Materials and methods

Isolation and culture of bovine chromaffin cells

Bovine adrenal glands were obtained from a local slaughterhouse. Chromaffin cells were isolated by digestion of the adrenal medulla with collagenase following standard methods [39] with some modifications [50]. Cells were suspended in Dulbecco's modified Eagle's medium (DMEM) supplemented with 5% fetal calf serum, 10 μM cytosine arabinoside, 10 μM fluorodeoxyrudine, 50 IU mL^{-1} penicillin, and 50 μg mL^{-1} streptomycin. Cells were plated on 13-mm diameter polylisine-coated glass coverslips at a density of 5×10^4 cells per coverslip. Cells were kept in a water-saturated incubator at 37°C in a 5% CO_2–95% air atmosphere and used 2–5 days thereafter.

Electrophysiological recordings

I_{Ca} were recorded in voltage-clamped cells under whole-cell configuration (WCC) or perforated-patch configuration (PPC) [26, 34] of the patch-clamp technique [29]. During recording, cells were continuously perfused (at a rate of 1 mL min^{-1}) with an external solution containing (in millimolar): 145 NaCl, 1.2 $MgCl_2$, 2 $CaCl_2$, 10 glucose, and 10 HEPES, pH adjusted to 7.4 with NaOH. In some experiments, equimolar Ba^{2+} was used instead of Ca^{2+} as charge carrier. For perforated-patch experiments, electrodes were filled with internal solution containing the following (in millimolar): 135 CsGlutamate, 10 HEPES, 1 $MgCl_2$, and 9 NaCl, pH 7.2 adjusted with CsOH. For this configuration, an amphotericin B stock solution was prepared every week at 50 mg mL^{-1} in dimethyl sulfoxide (DMSO), stored at −20°C, and protected from light. Fresh perforated-patch pipette solution was prepared every day by addition of 10 μL stock amphotericin B solution to 1 mL intracellular solution. This solution was sonicated thoroughly, protected from light, and kept in ice. Patch pipettes had their tips dipped in amphotericin-free solution for 2–10 s and backfilled with freshly mixed amphotericin-containing solution. For whole-cell experiments, cells were dialysed with an internal solution containing (in millimolar): 10 NaCl, 100 CsCl, 20 TEA-Cl, 14 EGTA, 20 HEPES, 5 MgATP, and 0.3 NaGTP, pH 7.2 adjusted with CsOH. When necessary, EGTA was omitted from the internal solution. For PPC, recordings started when the access resistance decreased below 25 MΩ, which usually happened within 10 min after sealing [61]. For WCC, the total pipette access resistance ranged from 2 to 3 MΩ.

Electrophysiological data were carried out using an EPC-9 amplifier under the control of Pulse software (HEKA Elektronik). Cells were held at −80 mV and I_{Ca} were generated by depolarizing voltage steps of 50-ms duration to sequentially increasing test potentials by 10-mV step increments from −50 to +50 mV. Test pulses were delivered at 10-s intervals to minimize the rundown of Ca^{2+} currents [16]. Cells with pronounced rundown were discarded. External solutions were exchanged by a fast superfusion device consisting of a modified multibarrelled pipette, the common outlet of which was positioned 50–100 μm from the cell. Control and test solutions were changed using miniature solenoid valves operated manually.

To determine the effects of L-type Ca^{2+} channel agonists under WCC or PPC, cells were perfused with external solutions containing either FPL (in most experiments) or BayK8644 (BayK; in a few experiments). All experiments were performed at room temperature (24±2°C).

Materials and solutions

The following materials were used: collagenase type I from Sigma (Madrid, Spain); DMEM, bovine serum albumin fraction V, fetal calf serum, and antibiotics were from Gibco (Madrid, Spain). Amphotericin B and BayK were from Sigma (Madrid, Spain) and FPL was from RBI (Natick, MA, USA); ω-conotoxin MVIIC (MVIIC) was from Bachem Feinchemikalien (Essex, UK).

FPL at 1 mM was prepared in ethanol and BayK at 1 mM in DMSO; both solutions were kept at −20°C in aliquots and were protected from light. MVIIC was dissolved in distilled water and stored frozen in aliquots at 0.1 mM. Final concentrations of drugs were obtained by diluting the stock solution directly into the external solution.

Data analysis

Under the appropriate conditions, FPL gradually augmented I_{Ca} along the 50-ms test depolarizing pulse (Fig. 1b). Therefore, the amplitude of I_{Ca} was always measured at the end of the test pulse (see double arrowheads in Fig. 1a). In order to measure the component of the tail current that occurred in the presence of L-type Ca^{2+} channel agonists, a second cursor was approximately placed 5 ms after the end of the test pulse. I_{Ca} was not leak subtracted, and only cells with a leak current <30 pA were included in the analysis. Comparisons between means of group data were performed by one-way analysis of variance followed by Duncan post hoc test when appropriate. A p value equal to or smaller than 0.05 was taken as the limit of significance. Data are expressed as means ± standard error (SE).

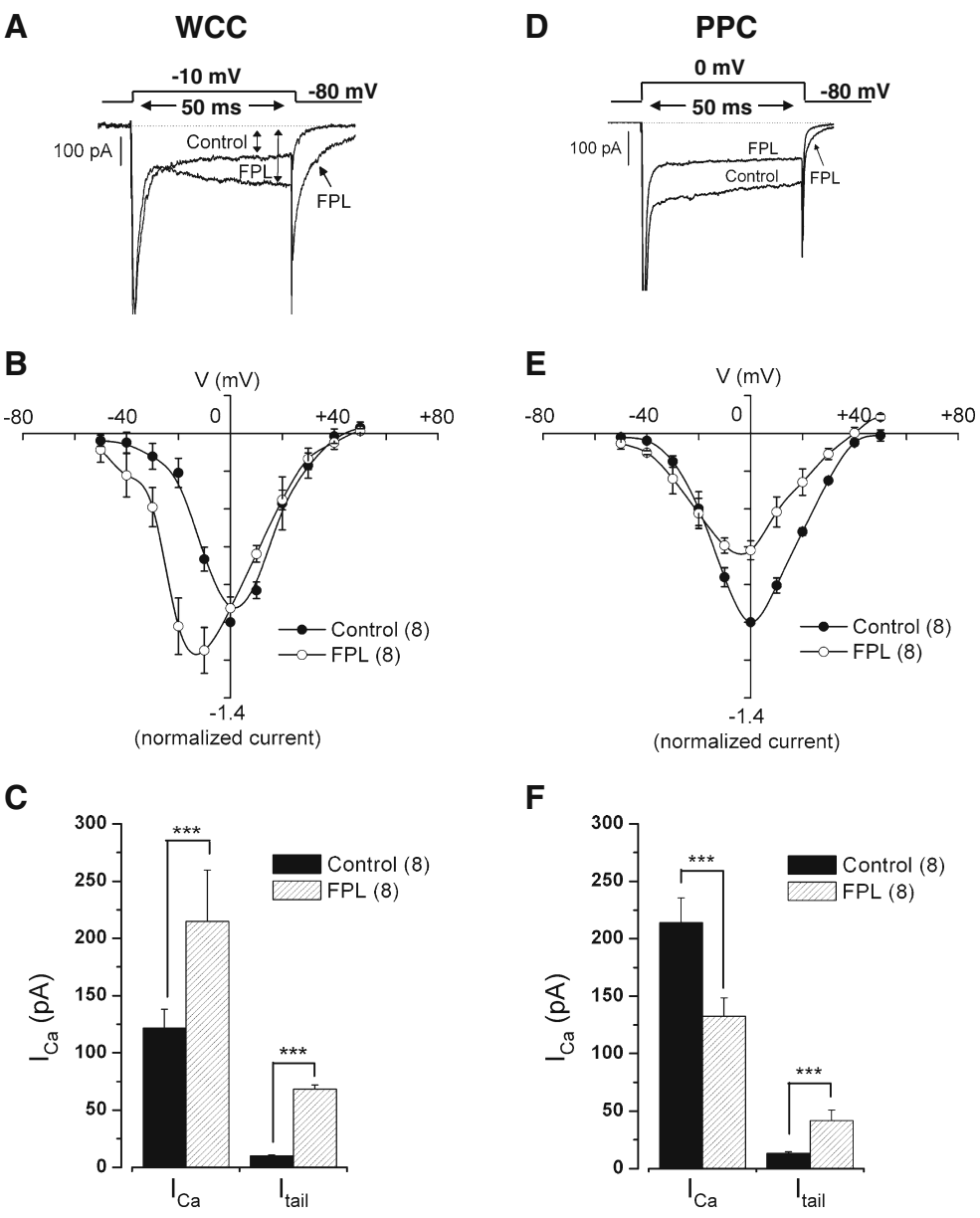

Fig. 1 FPL (1 μM) augmented I_{Ca} under WCC recording (**a**–**c**) and inhibited I_{Ca} under PPC recording (**d**–**f**). HP −80 mV; 2 mM external Ca^{2+}. **a**, **d** Example trace currents generated by test pulses to the voltages indicated at the protocol on top, before (control) and at 2 min of FPL treatment. **b**, **e** *I–V* relationship of I_{Ca}, before (control) and during FPL treatment. These curves were obtained by measuring I_{Ca} amplitude at the end of the test pulse (see *double arrowhead* in **a**); currents were generated by successive test potentials given at increasing 10-mV steps from −50 to +50 mV. **c**, **f** Pooled results of I_{Ca} amplitude (measured as indicated by the *double arrowhead* in **a**) and I_{tail} (measured at 5 ms after returning to HP −80 mV). Data are means ± SE of eight cells for each configuration, from at least four different cultures. ***p<0.001

Results

FPL augmented I_{Ca} under WCC but caused its inhibition under PPC

The fact that FPL increases $^{45}Ca^{2+}$ uptake into K^+ depolarized bovine chromaffin cells [70] suggested that the compound should also augment I_{Ca} in these cells. This $^{45}Ca^{2+}$ increase was maximal at 1 μM FPL; therefore, we used this concentration throughout this study. Generally, when a good seal was established in each experiment and access to the intracellular milieu was achieved, the targeted cell was voltage-clamped at −80 mV holding potential (HP). Then the cell was continuously perfused with an extracellular solution containing the physiological Ca^{2+} concentration of 2 mM. Unless otherwise indicated, under WCC recording, the pipette solution contained 14 mM EGTA; these are the conditions used in our and many other laboratories to prevent Ca^{2+} channel inactivation and optimize the recording of reproducible I_{Ca} current traces along the experiment. Under PPC recording, there was no point in adding EGTA to the pipette solution since this compound will not cross the perforated-patch pores; these are also the conditions thoroughly used to record I_{Ca} under PPC. In general, cells with leak currents greater than 30 pA were discarded (under WCC recording). Cells were usually challenged with test potentials given at different voltages at 10-s intervals.

In the example cell of Fig. 1a, a 50-ms pulse to −10 mV generated an inward current composed of (1) an initial fast-inactivating Na^+ current (we did not use tetrodotoxin in this study; however, the presence of 1 mM TTX fully suppressed the I_{Na} component of current traces); this current was large and, therefore, it appears truncated to facilitate the visualization of I_{Ca}; (2) a low-inactivating I_{Ca}; and (3) a deactivating tail current (I_{tail}) caused by Ca^{2+} channel closing upon returning to −80 mV (see protocol on top of Fig. 1a). After 1-min of perfusion with FPL, the current increased along the depolarizing pulse and was followed by an I_{tail} with a pronounced slowing down of current relaxation to zero baseline. These are typical effects of FPL on L channels [38, 42]. The characteristic effect of FPL on I_{Ca} suggested the convenience of expressing all quantitative data by measuring I_{Ca} at the end of the test pulse, as indicated by double arrowheads in the current traces of Fig. 1a. In this manner, when using the term I_{Ca} throughout this study, we mean the amplitude of I_{Ca} at the end of the test pulse. I_{tail} is the amplitude of the tail current measured 5 ms after the end of the test pulse in each cell. Figure 1b shows the typical shift to the left of the current–voltage (*I–V*) curve caused by activators of L channels [35, 75]. FPL augmented I_{Ca} only at steps in the negative range of the voltage scale. Figure 1c contains a summary of the averaged changes elicited by FPL: I_{Ca} augmented by 76% and I_{tail} by 5.8-fold.

A quite different picture emerged when I_{Ca} was recorded under PPC. I_{Ca} was halved when the example cell shown in Fig. 1d was treated with FPL; a tiny slowing down of I_{tail} was noted. FPL did not shift the *I–V* curve and caused its depression with respect to the control curve (Fig. 1e). The averaged data of Fig. 1f indicate that although FPL decreased I_{Ca} by 38%, I_{tail} was still augmenting 2.2-fold. This suggested that, in spite of I_{Ca} inhibition, FPL was still enhancing the open time of L channels.

In conclusion, under WCC recording, FPL augmented I_{Ca} and I_{tail} in the expected direction for an L Ca^{2+} channel activator. In contrast, under PPC recording, FPL blocked I_{Ca} and caused a lesser I_{tail} increase.

BayK mimicked the effects of FPL on I_{Ca}

BayK is the prototype L channel ligand that has been widely used since its discovery [65] as a tool to prolong the mean open time of such channel [57]. BayK drastically augments $^{45}Ca^{2+}$ uptake into K^+ depolarized bovine chromaffin cells [24]. Under these premises, we thought that BayK (a DHP derivative) should mimic the effects of FPL (a non-DHP derivative) on I_{Ca} and I_{tail}. We, therefore, performed experiments with designs similar to those used with FPL. As for FPL [70], we used 1 μM BayK, a concentration that maximally augments Ca^{2+} entry through Ca^{2+} channels in bovine chromaffin cells [24].

Under WCC, BayK augmented I_{Ca} and I_{tail} in the expected direction (Fig. 2a). The compound also shifted to the left the *I–V* curve by about 10 mV. Thus, BayK enhanced I_{Ca} at steps in the negative range of the voltage scale and depressed it in the positive range (Fig. 2b). This was similar to FPL that augmented I_{Ca} at negative voltage steps and mildly depressed it at positive steps (Fig. 1b). BayK augmented peak I_{Ca} by 61% and I_{tail} by 3.3-fold (Fig. 2c).

Under PPC recording, BayK had effects opposite to those found under WCC (Fig. 1). For instance, in the example trace of Fig. 2d, BayK caused a mild inhibition of I_{Ca}, and did not augment I_{tail}. The *I–V* curve underwent a meager depression with no shift (Fig. 2e). The averaged results indicate a 24% blockade of I_{Ca} and no effect on I_{tail} (Fig. 2f).

In conclusion, from a qualitative point of view, BayK affected I_{Ca} in a direction similar to FPL: augmentation under WCC recording and diminution under PPC. However, from a quantitative point of view, the effects of BayK were milder; therefore, we chose FPL to perform further experiments.

FPL enhanced I_{Ca} under both WCC and PPC recordings in conditions of L current isolation

As indicated in the Introduction section, we depart from the hypothesis that Ca^{2+} entry through L channels causes the

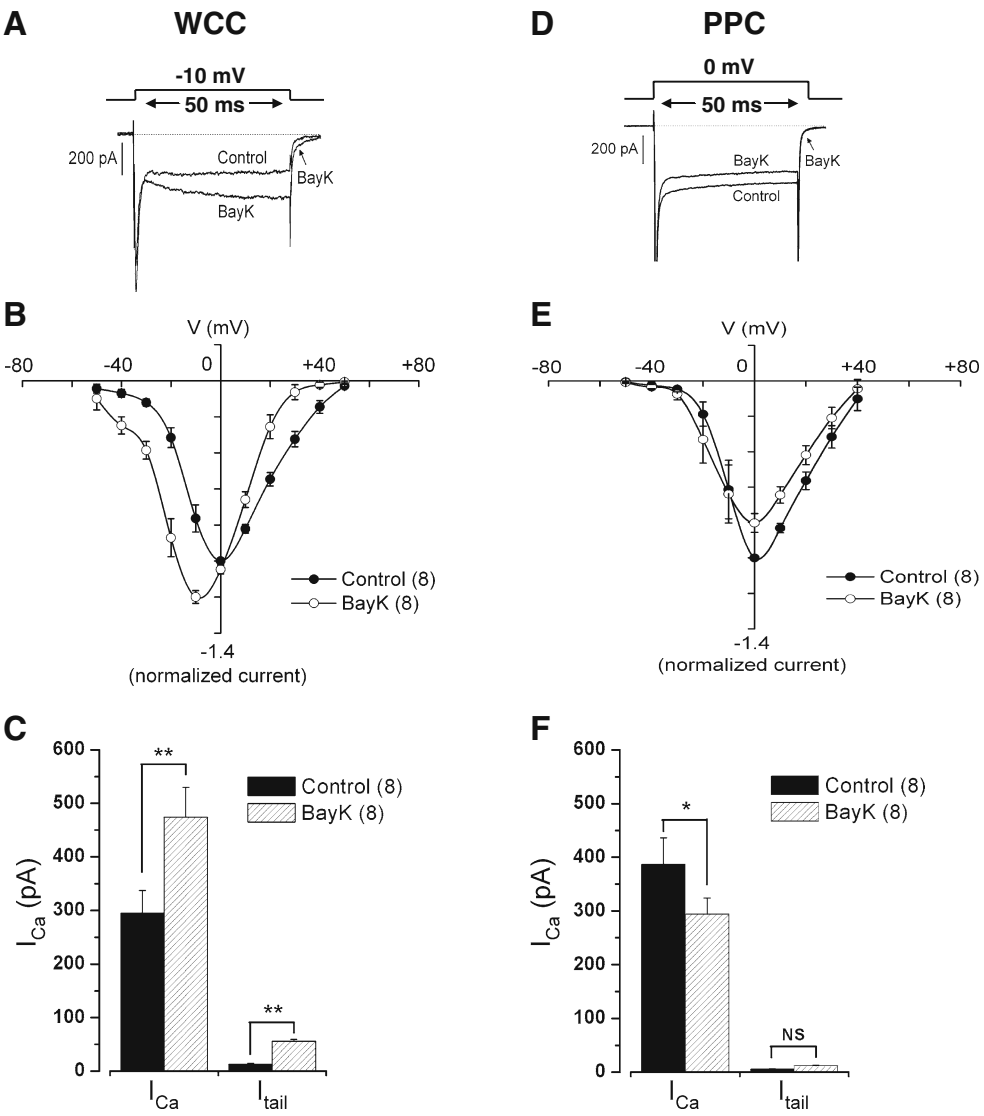

Fig. 2 BayK (1 μM) augmented I_{Ca} under WCC recording (**a**–**c**) and inhibited I_{Ca} under PPC recording (**d**–**f**). HP −80 mV; 2 mM external Ca^{2+}. **a**, **d** Example trace currents generated by test pulses to the voltages indicated at the protocol on top, before (control) and at 2 min of BayK treatment. **b**, **e** *I–V* relationship of I_{Ca}, before (control) and during BayK treatment. These curves were obtained by measuring I_{Ca} amplitude at the end of the test pulse; currents were generated by successive test potentials given at increasing 10-mV steps from −50 to +50 mV. **c**, **f** Pooled results of I_{Ca} and I_{tail} amplitudes. Data are means ± SE of eight cells for each configuration, from at least four different cultures. *$p<0.05$, ***$p<0.001$. *NS* nonsignificant

inhibition of N and PQ channels. In bovine chromaffin cells, L channel current accounts for only 20% of the whole-cell current; the rest is carried through N and PQ channels [2, 18, 40]. In these cells, 2 μM MVIIC suppresses the N and PQ components of the whole-cell inward current through Ca^{2+} channels [19]. Therefore, we recoursed to 2 μM MVIIC to block N and PQ currents, leaving the cell with its L current intact.

Under WCC recording, MVIIC inhibited I_{Ca} by 43%, as exemplified in the original traces of Fig. 3a (inset i). When added on top of MVIIC, FPL augmented I_{Ca} and slowed down the relaxation of I_{tail} (inset ii) to near the control level. On the other hand, MVIIC depressed the *I–V* curve; when added with MVIIC, FPL shifted to the left the *I–V* curve and thus augmented I_{Ca} at step potentials in the negative voltage scale (Fig. 3b). The averaged I_{Ca} changes appear in Fig. 3c. MVIIC reduced I_{Ca} by 58% in the presence of the toxin, FPL augmented I_{Ca} to about 70% of the initial control current.

Under PPC recording, MVIIC reduced I_{Ca} by 67% in the example cell shown in Fig. 3d. When added on top of MVIIC, FPL augmented I_{Ca} and delayed I_{tail} relaxation (see inset ii in Fig. 3d). MVIIC depressed the *I–V* curve in a parallel manner. When added together with MVIIC, FPL augmented I_{Ca} to about 70% of the initial control *I–V* curve (Fig. 3e). Averaged results are summarized in Fig. 3f; I_{Ca} was inhibited 80% by MVIIC. Although this inhibited current was doubled by FPL, this increase was not significantly different.

Another way of isolating the L from N/PQ currents rests on the voltage-dependent inactivation of N/PQ channels. Shifting of the HP from −80 to −50 mV causes the gradual loss of 70–80% of current; the remaining current is blocked by nifedipine and is thus associated to noninactivating L channels [31, 70]. This was reproduced here under WCC

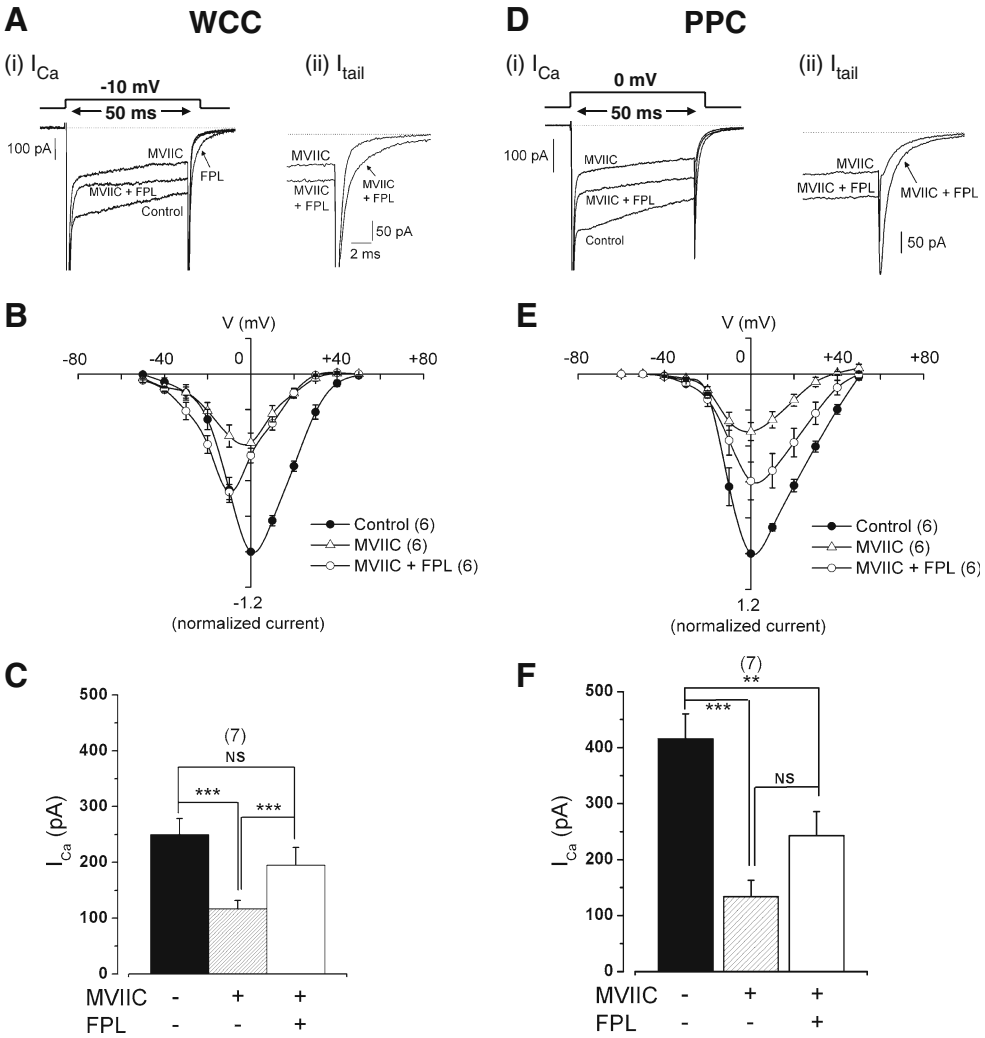

Fig. 3 FPL (1 μM) augmented I_{Ca} and I_{tail} under conditions of WCC recording (**a**–**c**) and PPC recording (**d**–**f**) in cells treated with ω-conotoxin MVIIC (MVIIC, 2 μM) to suppress N and PQ Ca^{2+} channel currents. HP −80 mV; 2 mM external Ca^{2+}. **a**, **d** Example trace currents generated by test pulses to the voltages indicated at the protocol on top, before (control), at 2 min of MVIIC treatment, and at 2 min of combined MVIIC + FPL treatment. **b**, **e** *I–V* relationship of I_{Ca}, during MVIIC treatment and during MVIIC + FPL treatment. These curves were obtained as described in Fig. 1. **c**, **f** Pooled results of I_{Ca} and I_{tail} amplitudes. Data are means ± SE of six cells for each configuration, from at least three different cultures. *p< 0.05, **p<0.01, ***p<0.001

recording. In the example cell shown in Fig. 4a, I_{Ca} declined to about 30% of initial current upon switching the HP from −80 to −50 mV. FPL gradually augmented I_{Ca} as well as I_{tail} to reach a plateau in about a minute. Current traces from this time course curves (a, b, c) are shown in Fig. 4b; note the progressive augmentation of I_{Ca} (i) and the drastic slowing down of I_{tail} relaxation (ii). Pooled data (Fig. 4c) indicate a voltage-dependent current loss of 54% and its augmentation to about 60% of the initial I_{Ca} upon FPL treatment. Particularly impressive was the eightfold increase of I_{tail}.

Under PPC recording, the reduction of I_{Ca} was also gradual and stabilized after a couple of minutes at −50 mV HP (Fig. 4d). FPL gradually augmented I_{Ca} and I_{tail} to reach a plateau after about 2 min. The example traces shown in Fig. 4e show the mild FPL-induced I_{Ca} increase (i) and the more pronounced slowing down of I_{tail} relaxation (ii). Pooled data (Fig. 4f) show a 60% decrease of I_{Ca} at −50 mV HP and 37% increase elicited by FPL with fivefold augmentation of I_{tail}.

In conclusion, under conditions of L current isolation, either with MVIIC or depolarized HP, FPL equally augmented I_{Ca} and I_{tail} under WCC and PPC recording conditions. This contrasts with the results obtained when I_{Ca} flows through all channel types where FPL augmented I_{Ca} under WCC recording but caused its inhibition under PPC. It seems, therefore, that this inhibition must be associated to N/PQ channels, rather than L channels.

The presence or absence of EGTA in the cytosol modifies the effects of FPL under WCC and PPC recordings

Under WCC recording, the intracellular solution contained 14 mM EGTA. Under these conditions, Ca^{2+} entering through Ca^{2+} channels will be chelated, the $[Ca^{2+}]_c$ will not increase, and the Ca^{2+}-dependent inhibition of Ca^{2+} channels will be prevented [32]. We, therefore, expected that an experiment performed in conditions similar to those of Fig. 1 under WCC recording, but using an intracellular

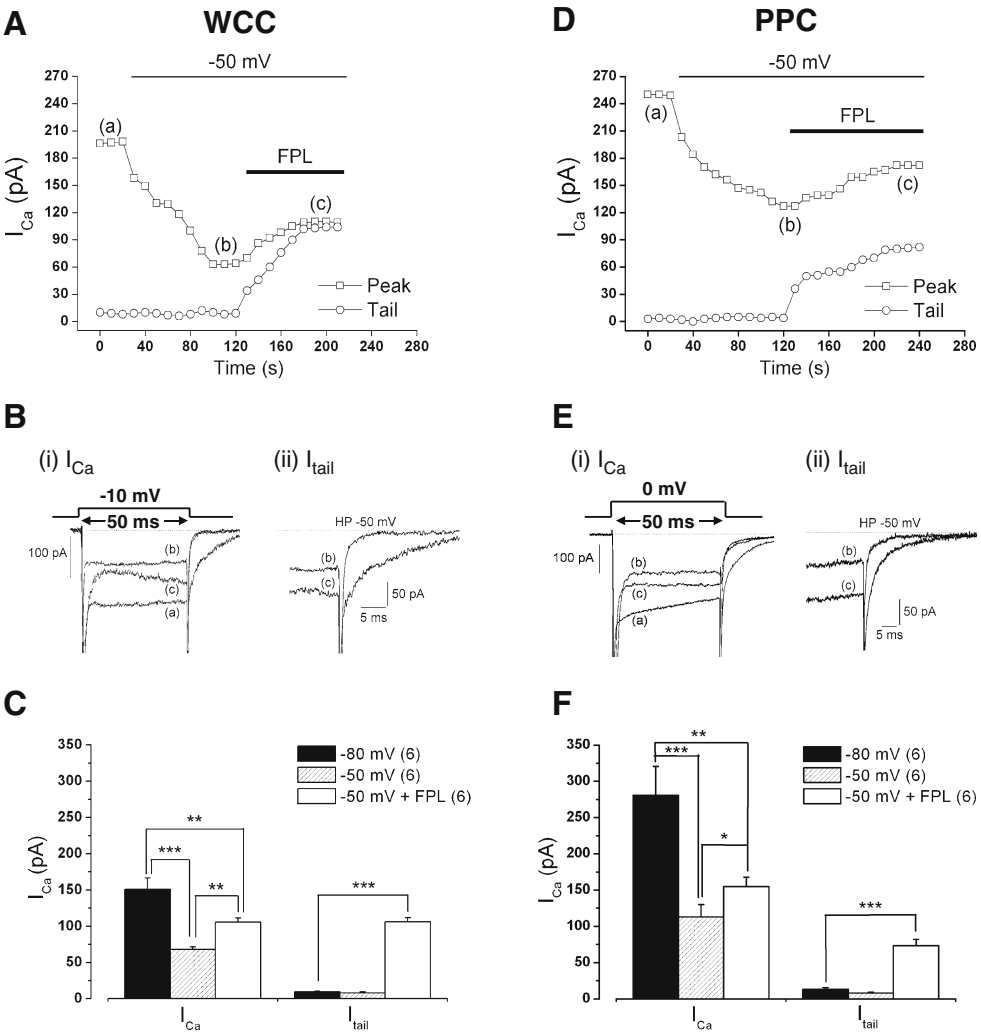

Fig. 4 FPL (1 μM) augmented I_{Ca} and I_{tail} under conditions of WCC recording (**a**–**c**) and PPC recording (**d**–**f**) in cells voltage-clamped at −50 mV in order to suppress N and PQ Ca^{2+} channel currents. HP was initially maintained at −80 mV; subsequently, HP was switched to −50 mV as indicated by the *horizontal bars on top* of **a** and **d**; 2 mM Ca^{2+} was present in the extracellular solution. **a**, **d** Time courses of I_{Ca} and I_{tail}. FPL was perfused during the time period indicated by the *horizontal bars*. Test pulses to −10 mV were applied at 10-s intervals. **b**, **e** Example I_{Ca} (*i*) and I_{tail} currents (*ii*) taken from experiments of **a** and **d** at the times indicated by **a**–**c**. **c**, **f** Pooled results on I_{Ca} and I_{tail} amplitudes calculated at the HP indicated and after 2 min perfusion with FPL. Data are means ± SE of six cells for each configuration, from at least three different cultures. *p<0.05, **p<0.01, ***p<0.001

solution deprived of EGTA, will favor the inhibition of N/PQ channel current.

The example I_{Ca} traces of Fig. 5a show that FPL inhibits I_{Ca} by 36% at a test potential of 0 mV and by 49% at +10 mV. There was a tiny slowing down of I_{tail}, particularly at +10 mV. This inhibition was seen only at depolarizing test potentials, as shown by the *I–V* curves of Fig. 5b. Pooled data indicate that the initial I_{Ca} of 350 pA was reduced 45% by FPL. This was a picture quite similar to that found under PPC recording with no EGTA in the cytosol (compare the *I–V* curves of Figs. 1e and 5b).

Under PPC recording, EGTA could not be given in the pipette solution because it will not cross the pores of the perforated membrane patch. Hence, we recourse to the cell-permeable EGTA-AM to load the cell cytosol with EGTA before doing the experiment. Figure 5d shows example I_{Ca} traces; a tiny augmentation of I_{Ca} and I_{tail} were seen upon FPL treatment both at −10 and 0 mV test potentials. FPL shifted the *I–V* curve to the left, indicating that FPL augmented I_{Ca} only at hyperpolarizing potentials (Fig. 5e). Pooled data show that FPL augmented I_{Ca} by 33% (Fig. 5f). These FPL effects were quite similar to those found under WCC recording with EGTA in the cytosol (compare the *I–V* curves of Figs. 1b and 5b).

In conclusion, under WCC, EGTA removal from the patch pipette turned FPL-induced I_{Ca} augmentation into inhibition; conversely, under PPC, the presence of EGTA in the cytosol converted FPL-induced I_{Ca} inhibition into potentiation. This supports the view that Ca^{2+}-dependent inactivation by Ca^{2+} entry through L channels is responsible for the inhibition of the fraction of the current carried through non-L channels.

Effects of FPL on Ca^{2+} channel currents using Ba^{2+} (instead of Ca^{2+}) as charge carrier, under WCC and PPC recordings

The Ca^{2+} inactivation of Ca^{2+} channels is prevented when using Ba^{2+} (instead of Ca^{2+}) as charge carrier. This is true for neurons [27] as well as bovine chromaffin cells [7, 72].

By using 2 mM Ba^{2+} (instead of 2 mM Ca^{2+}) as charge carrier, we expected to find similar effects of FPL on Ba^{2+} currents (I_{Ba}), under both WCC and PPC recordings.

Figure 6a shows example I_{Ba} traces obtained under WCC recording. FPL augmented I_{Ba} by 90% and caused a pronounced delay of I_{tail} relaxation. FPL shifted the entire *I–V* curve to the left, indicating I_{Ba} augmentation at steps in the negative range of the voltage scale and inhibition in the positive range (Fig. 6b). Pooled results show that FPL augmented I_{Ba} by 90% and I_{tail} by as much as sixfold (Fig. 6c).

Under PPC recording, the data came in a similar direction. For instance, the example traces of Fig. 6d show a progressive augmentation of I_{Ba} along the depolarizing pulse and a pronounced slowing down of the tail current. However, the *I–V* curve was shifted to the left only in the negative range of the voltage scale where I_{Ba} was augmented by FPL (Fig. 6e). Pooled results indicate that FPL enhanced I_{Ba} by 80% and I_{tail} by as much as sevenfold (Fig. 6f).

In conclusion, FPL modified I_{Ba} (peak and tail currents) in a similar way, irrespective of whether the recordings were made under WCC or PPC.

Discussion

The central finding of this study was that FPL, an enhancer of Ca^{2+} entry through L-type Ca^{2+} channels, caused a paradoxical inhibition of the whole-cell inward current flowing through Ca^{2+} channels during depolarization of voltage-clamped bovine chromaffin cells. Such inhibition was initially observed only under PPC recording since, under WCC recording, FPL augmented I_{Ca} and I_{tail} in the expected direction. We later on found that these opposing FPL actions could be explained by the absence or the presence of the mobile Ca^{2+} buffer EGTA in the intracellular solution used under PPC or WWC recordings, respectively.

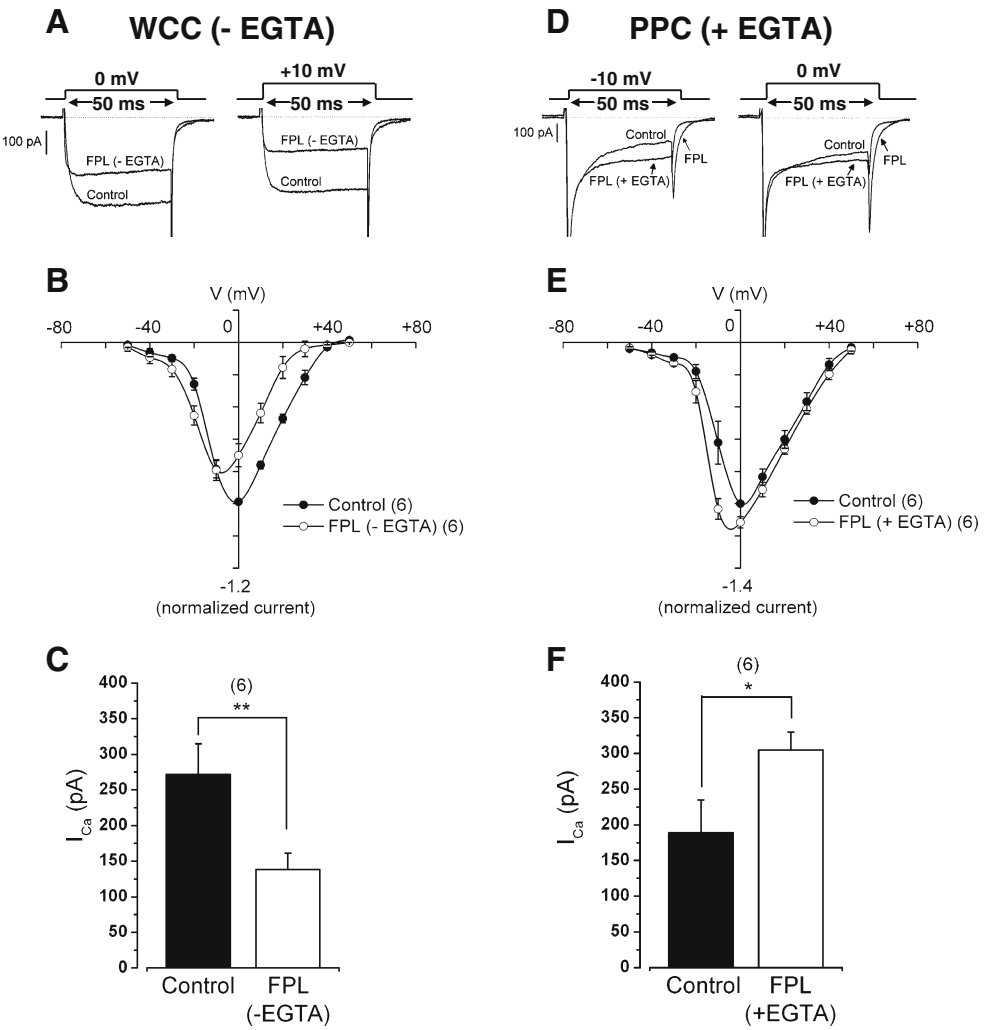

Fig. 5 Effects of EGTA on the changes of I_{Ca} elicited by FPL under WCC recording (**a**–**c**) and PPC recording (**d**–**f**) recording conditions. HP −80 mV; 2 mM external Ca^{2+}. Under WCC recording, the pipette solution contained no EGTA; under PPC recording, before the experiment, cells were incubated during 45 min with cell permeable EGTA-AM at 37°C. Cells were subsequently washed during 15 min at room temperature with the extracellular solution. Then, the cells were patched and the experiments were performed as usual under PPC recording. **a**, **d** Example trace currents generated by test pulses to the voltages indicated at the protocol on top, before (control) and at 2 min of FPL treatment. **b**, **e** *I–V* relationship of I_{Ca}, before (control) and during FPL treatment. **c**, **f** Pooled results on the effects of FPL on I_{Ca} (measured at 0 mV test potential). Data are means ± SE of six cells for each configuration, from at least three different cultures. *$p<0.05$, **$p<0.01$

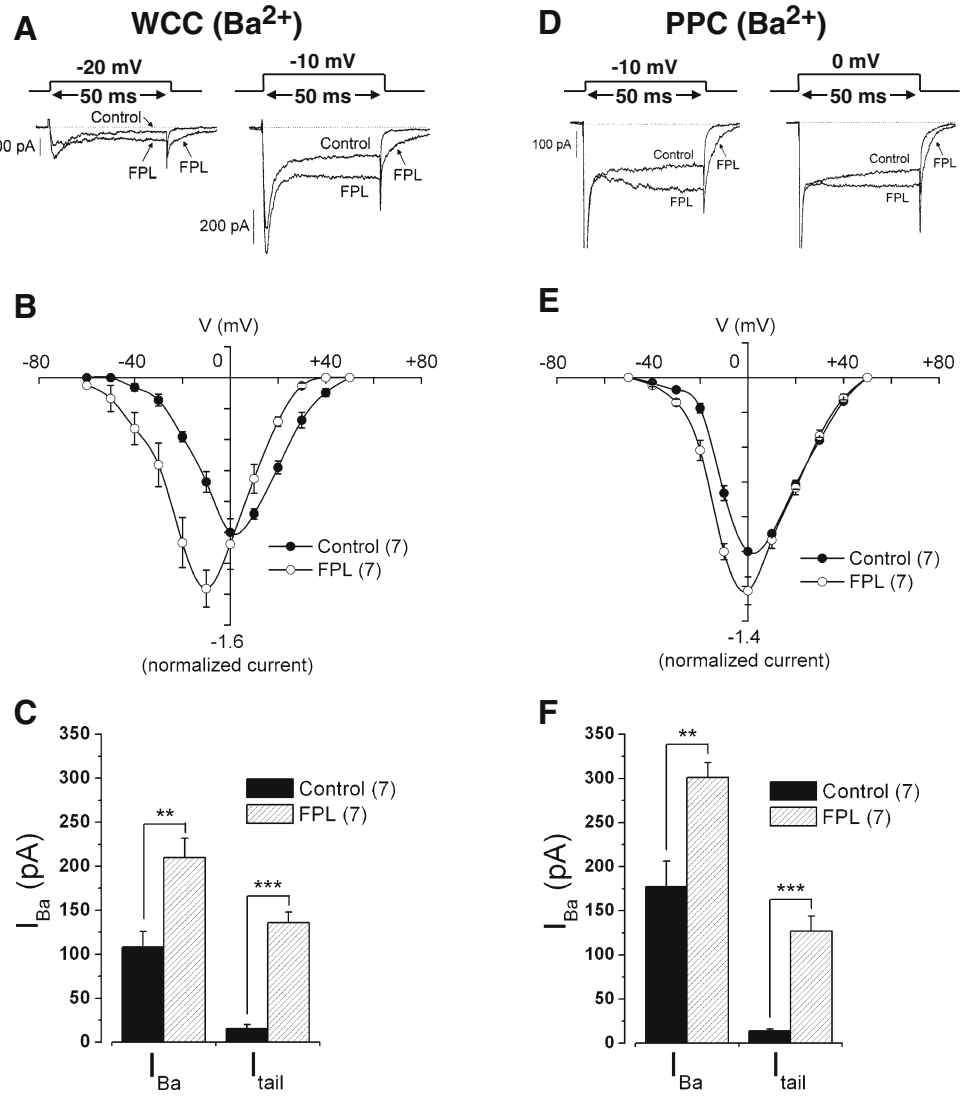

Fig. 6 FPL (1 μM) augmented I_{Ca} under both WCC (**a**–**c**) and PPC recording (**d**–**f**) if 2 mM Ba^{2+} (instead of 2 mM Ca^{2+}) was used as charge carrier. HP −80 mV; 2 mM external Ba^{2+}. **a**, **d** Example trace currents generated by test pulses to the voltages indicated at the protocol on top, before (control) and at 2 min of FPL treatment. **b**, **e** *I–V* relationship of I_{Ba}, before (control) and during FPL treatment. These curves were made as indicated in Fig. 1. **c**, **f** Pooled results of I_{Ba} and I_{tail} amplitudes before and during FPL treatment. Data are means ± SE of seven cells for each configuration, from at least three different cultures. $^{**}p<0.01$, $^{***}p<0.001$

The initial observation on FPL-induced I_{Ca} blockade was done under PPC recording (Fig. 1d). Thus, the possibility existed that, under this patch-clamp configuration, FPL caused a direct pharmacological inhibitory effect on some or all of the major Ca^{2+} channels expressed by bovine chromaffin cells, i.e., L, N, and PQ [23]. In fact, at 10 μM, FPL inhibited the majority of the whole-cell current in HEK cells expressing N channels; however, at 1 μM, the concentration used in this study, FPL did not block the N current [38].

I_{Ca} inhibition by FPL may rather be explained in a different context. For instance, under PPC, when FPL inhibited I_{Ca} amplitude, I_{tail} remained enhanced (Fig. 1d, f). This indicates that FPL was indeed augmenting I_{Ca} through L channels. However, these channels carry only about 15–20% of the whole-cell I_{Ca} in bovine chromaffin cells, the rest being carried by N and PQ channels [2, 3, 17, 40]. Therefore, the inhibition by FPL of N/PQ current components could mask its enhancing effects on the L current component. This was demonstrated to be the case in the experiment where N/PQ currents were blocked by MVIIC (Fig. 3) or by maintaining the HP at −50 mV (Fig. 4). Under these conditions of L current isolation, FPL always augmented I_{Ca} and I_{tail} regardless of the recording conditions, WCC or PPC (Figs. 3 and 4).

Various experimental data support the view that FPL was not directly inhibiting the N/PQ currents; rather, such inhibition was indirectly associated to enhanced Ca^{2+} entry through L channels that were kept open longer in the presence of FPL, as the following facts suggest: (1) under PPC recording, the presence of cytosolic EGTA turned the I_{Ca} inhibition into an I_{Ca} augmentation (Fig. 5); (2) conversely, under WCC recording, EGTA removal from the intracellular solution turned the augmented I_{Ca} into a depressed I_{Ca} (Fig. 5); (3) when using Ba^{2+} as charge carrier, which does not inactivate Ca^{2+} channels [7, 27],

FPL augmented I_{Ba} under both WCC and PPC recordings. Thus, FPL-induced I_{Ca} inhibition did not depend on the patch-clamp configuration used but on whether the experimental conditions allowed an elevation of $[Ca^{2+}]_c$ during the application of depolarizing pulses. The possibility existed that the effects of FPL were linked to the washout of a cytosolic factor that is the target of the Ca^{2+}; such factor could be removed under WCC recording. We did experiments in six cells, recording under WCC from the beginning of seal rupture. I_{Ca} amplitude was gradually augmented from about 40 pA at the moment of seal rupture to about 140 pA in 1 min thereafter. FPL caused a pronounced I_{Ca} augmentation from the beginning of seal rupture but only in the presence of EGTA. This indicates that the washout of a cytosolic factor is not involved in the FPL effects of I_{Ca}.

Now the question arises as to whether the amount of Ca^{2+} entering the cell during brief depolarizing pulses (50 ms in our present study) is sufficient to build up a local $[Ca^{2+}]_c$ transient to inactivate N/PQ Ca^{2+} channels. The averaged $[Ca^{2+}]_c$ peaks measured with Ca^{2+} probes do not detect the high $[Ca^{2+}]_c$ transients occurring at subplasmalemmal sites during cell depolarization [13, 54, 67]. Using pulsed laser imaging, Monck and workers [45] visualized hot spots of submembranous Ca^{2+} evoked by 50 ms depolarizing pulses, the same stimulation pattern used in the present study. These hot spots developed in 20–50 ms and extended laterally by several micrometers. Partial or complete submembranous rings of elevated $[Ca^{2+}]$ appeared at 50–100 ms after channel opening, and the Ca^{2+} gradient collapsed at 200–400 ms after the pulse began. This was interpreted as due to a limited Ca^{2+} diffusion because of rapid Ca^{2+} sequestration by immobile buffers [45, 76].

In bovine chromaffin cells, the cytosol has a Ca^{2+} binding capacity of 4 mmol/L cells. The endogenous Ca^{2+} buffer is scarcely mobile, has a low affinity for Ca^{2+} ($k_d \sim 100$ μM) and an activity coefficient of ~1/40 [74, 76]. The two-dimensional diffusion coefficient is ~40 $\mu m^2/s$ and shows inhomogeneities at the plasma membrane [51]. Brief openings of VDCCs generate $[Ca^{2+}]_c$ microdomains as high as 10 or even 100 μM [8, 55]. Using mitochondria as biosensors for $[Ca^{2+}]_c$ changes, we found that ACh or K^+ pulses caused $[Ca^{2+}]_c$ elevations of 20–40 μM at subplasmalemmal sites of bovine chromaffin cells [47]. Because of rapid diffusion of Ca^{2+} towards the surrounding cytosol, these Ca^{2+} microdomains are very much restricted in time and space [53, 54]. The presence of mobile Ca^{2+} buffers accelerates diffusion and oppose the development of high $[Ca^{2+}]_c$ microdomains during cell depolarization [4, 5, 56, 64]. For instance, at 50 μM, a high-affinity low-capacity Ca^{2+} buffer such as fura-2 increases the apparent rate of Ca^{2+} diffusion by as much as four times [76].

In our present experiments, we dialyzed the cytosol with 14 mM EGTA under WCC recording or we incubated the cells with EGTA-AM for PPC experiments. Being a strong buffer [43], EGTA will prevent the buildup of high Ca^{2+} microdomains at subplasmalemmal sites during cell stimulation with 50 ms depolarizing pulses, as happened to be the case with fura-2 [76]. Under these conditions, it is understandable that Ca^{2+} induced N/PQ channel inhibition was not taking place and that the dominant FPL effects were I_{Ca} and I_{tail} increase and slowing down of I_{tail} due to L channel activation.

As discussed above, the bovine chromaffin cell cytosol contains strong Ca^{2+} buffers that severely restrict the diffusion of the Ca^{2+} entering through Ca^{2+} channels. Therefore, we must admit that, to cause inactivation of N/PQ channels, the Ca^{2+} has to enter the cell through L channels located close by. This effect might occur under physiological stimulation of chromaffin cells. However, it could better be unmasked by FPL-induced enhanced Ca^{2+} entry through L channels. From a functional point of view, this possible colocalization of L and non-L channels can be further investigated using FPL as a pharmacological tool to selectively augment Ca^{2+} entry through L channels. A challenging question to explore is whether L, N, and PQ channels form functional clusters units to regulate diverse exocytotic responses tailored to specific needs. In this context, it is interesting to note that some authors have found hot spots of Ca^{2+} entry and release in bovine chromaffin cells [62]. Furthermore, active exocytotic zones have been found in bovine chromaffin cells [66, 73] and a functional polarization of secretory sites have been revealed using confocal fluorescence microscopy, also in bovine chromaffin cells [12]. However, this clustering of Ca^{2+} channel subtypes at specific plasmalemmal sites makes it difficult to understand how the Ca^{2+} entering through a given channel type may have a selective function distinct from the Ca^{2+} entering through other channel type. Also, the question emerges on why Ca^{2+} entering through N/PQ channels (about 80% of the I_{Ca}) is not eliciting the inactivation of such channels. Unfortunately, compounds that prevent the inactivation of N/PQ channels (as the case is for L channels with FPL and BayK) are not available to help answer these questions. Further insight into the possible colocalization of Ca^{2+} channel subtypes could be achieved through the judicious use of various concentrations of EGTA (slow Ca^{2+} chelator) and BAPTA (rapid Ca^{2+} chelator). This approach has been useful to study Ca^{2+} channel colocalization with the secretory machinery (reviewed in García et al. [23]). However, the extrapolation of this strategy to demonstrate colocalization of Ca^{2+} channel subtypes may be difficult in the context of the present experiments. Immunofluorescence experiments with specific antibodies for α1 subunits of L, N, and P/Q channels could also provide some information on the possible colocalization of these channels. An alternative

explanation may be linked to the different molecular mechanisms underlying the regulation of Ca^{2+} channel subtypes by the Ca^{2+}-binding protein calmodulin and/or intracellular messengers [11, 15, 37, 49]. It may be that the lower Ca^{2+} affinity of calmodulin lobe or another lower affinity Ca^{2+}-binding protein experiences activating concentrations in the microdomains around isolated L channels and then dissociates and travels to affect N/PQ channels.

Finally, the possible specialization of the various Ca^{2+} channel subtypes expressed within the same cell to perform specific functions deserves a comment. Since the discovery that bovine chromaffin cells expressed multiple Ca^{2+} channels, efforts have been made to find out a kind of specialization for each channel subtype to drive a specific cell function. For instance, concerning exocytosis, L channels [6, 33], PQ channels [36], or all channels [41, 69] drive the secretory process. This disparity may be due to different stimuli and experimental conditions used [23]. The possible specialization of Ca^{2+} channel subtypes in bovine chromaffin cells has been explored in functional aspects other than exocytosis. For instance, Ca^{2+} entry through L channels, but not through N and PQ channels, causes mitochondrial disruption and cell death by apoptosis [10]; also, Ca^{2+} entry through L channels are preferentially coupled to endocytosis [60, 63]. However, other studies do not attribute a special function to a given channel subtype. This is the case for tyrosine hydroxylase activation [58], SNAP-25 expression [21], ERK phosphorylation [48], or mitochondrial Ca^{2+} uptake [46]; these studies concluded that these cell functions depended more on critical $[Ca^{2+}]_c$ levels than on Ca^{2+} entry through a given Ca^{2+} channel subtype. The results of our present study, however, clearly indicate that the Ca^{2+} entering through L channels have a clear-cut function, the modulation of N and PQ channel activities during cell depolarization. To our knowledge, this is the first report suggesting this function for the L-type voltage-dependent Ca^{2+} channel.

To conclude, the L-type Ca^{2+} channel activator FPL caused opposing effects on I_{Ca}, i.e., augmentation under WCC recording and inhibition under PPC recording. The experiments done in this study to clarify these apparent paradoxical effects suggest that Ca^{2+} entry through L channels causes a Ca^{2+}-dependent inhibition of N and PQ channels. FPL seems to be a good tool to further explore functional aspects of this novel regulatory action of Ca^{2+} flux through L-type channels.

Acknowledgements This work was supported by grants from Ministerio de Ciencia e Innovación (SAF2006-03589 to AGG; SAF2007-65181 to LG); Instituto de Salud Carlos III (RETICS-RD06/0026); Comunidad Autónoma de Madrid (S-SAL-0275-2006); and Fundación Mutua Madrileña (to AGG and LG). JMR is a fellow of FPU program, Universidad Autónoma de Madrid, Spain. We thank Lorena Cortés and Inés Colmena for the preparation of excellent cell cultures and the "Fundación Teófilo Hernando" for the continued support.

References

1. Albillos A, Carbone E, Gandia L, Garcia AG, Pollo A (1996) Opioid inhibition of Ca^{2+} channel subtypes in bovine chromaffin cells: selectivity of action and voltage-dependence. Eur J Neurosci 8:1561–1570
2. Albillos A, Garcia AG, Gandia L (1993) omega-Agatoxin-IVA-sensitive calcium channels in bovine chromaffin cells. FEBS Lett 336:259–262
3. Albillos A, Garcia AG, Olivera B, Gandia L (1996) Re-evaluation of the P/Q Ca^{2+} channel components of Ba^{2+} currents in bovine chromaffin cells superfused with solutions containing low and high Ba^{2+} concentrations. Pflugers Arch 432:1030–1038
4. Alonso MT, Montero M, Carnicero E, Garcia-Sancho J, Alvarez J (2002) Subcellular Ca^{2+} dynamics measured with targeted aequorin in chromaffin cells. Ann N Y Acad Sci 971:634–640
5. Alonso MT, Villalobos C, Chamero P, Alvarez J, Garcia-Sancho J (2006) Calcium microdomains in mitochondria and nucleus. Cell Calcium 40:513–525
6. Artalejo CR, Adams ME, Fox AP (1994) Three types of Ca^{2+} channel trigger secretion with different efficacies in chromaffin cells. Nature 367:72–76
7. Artalejo CR, Garcia AG, Aunis D (1987) Chromaffin cell calcium channel kinetics measured isotopically through fast calcium, strontium, and barium fluxes. J Biol Chem 262:915–926
8. Augustine GJ, Neher E (1992) Calcium requirements for secretion in bovine chromaffin cells. J Physiol 450:247–271
9. Brehm P, Eckert R (1978) Calcium entry leads to inactivation of calcium channel in Paramecium. Science 202:1203–1206
10. Cano-Abad MF, Villarroya M, Garcia AG, Gabilan NH, Lopez MG (2001) Calcium entry through L-type calcium channels causes mitochondrial disruption and chromaffin cell death. J Biol Chem 276:39695–39704
11. Cens T, Rousset M, Leyris JP, Fesquet P, Charnet P (2006) Voltage- and calcium-dependent inactivation in high voltage-gated Ca^{2+} channels. Prog Biophys Mol Biol 90:104–117
12. Cuchillo-Ibáñez I, Michelena P, Albillos A, García AG (1999) A preferential pole for exocytosis in cultured chromaffin cells revealed by confocal microscopy. FEBS Lett 459:22–26
13. Chad JE, Eckert R (1984) Calcium domains associated with individual channels can account for anomalous voltage relations of CA-dependent responses. Biophys J 45:993–999
14. Chan SA, Polo-Parada L, Smith C (2005) Action potential stimulation reveals an increased role for P/Q-calcium channel-dependent exocytosis in mouse adrenal tissue slices. Arch Biochem Biophys 435:65–73
15. DeMaria CD, Soong TW, Alseikhan BA, Alvania RS, Yue DT (2001) Calmodulin bifurcates the local Ca^{2+} signal that modulates P/Q-type Ca^{2+} channels. Nature 411:484–489
16. Fenwick EM, Marty A, Neher E (1982) Sodium and calcium channels in bovine chromaffin cells. J Physiol 331:599–635
17. Gandía L, Albillos A, García AG (1993) Bovine chromaffin cells possess FTX-sensitive calcium channels. Biochem Biophys Res Commun 194:671–676
18. Gandía L, García AG, Morad M (1993) ATP modulation of calcium channels in chromaffin cells. J Physiol 470:55–72
19. Gandia L, Lara B, Imperial JS, Villarroya M, Albillos A, Maroto R, Garcia AG, Olivera BM (1997) Analogies and differences between omega-conotoxins MVIIC and MVIID: binding sites and functions in bovine chromaffin cells. Pflugers Arch 435:55–64
20. Gandía L, Montiel C, García AG, López MG (2008) Calcium channels for exocytosis: functional modulation with toxins. In: Botana L (ed) Seafood and freshwater toxins: pharmacology, physiology and detection. CRC Press, Boca Raton, FL, USA, pp 107–148

21. García-Palomero E, Montiel C, Herrero CJ, García AG, Alvarez RM, Arnalich FM, Renart J, Lara H, Cárdenas AM (2000) Multiple calcium pathways induce the expression of SNAP-25 protein in chromaffin cells. J Neurochem 74:1049–1058
22. García-Palomero E, Renart J, Andres-Mateos E, Solís-Garrido LM, Matute C, Herrero CJ, García AG, Montiel C (2001) Differential expression of calcium channel subtypes in the bovine adrenal medulla. Neuroendocrinology 74:251–261
23. García AG, García-De-Diego AM, Gandía L, Borges R, García-Sancho J (2006) Calcium signaling and exocytosis in adrenal chromaffin cells. Physiol Rev 86:1093–1131
24. García AG, Sala F, Reig JA, Viniegra S, Frias J, Fonteriz R, Gandía L (1984) Dihydropyridine BAY-K-8644 activates chromaffin cell calcium channels. Nature 309:69–71
25. Giannattasio B, Jones SW, Scarpa A (1991) Calcium currents in the A7r5 smooth muscle-derived cell line. Calcium-dependent and voltage-dependent inactivation. J Gen Physiol 98:987–1003
26. Gillis KD, Pun RY, Misler S (1991) Long-term monitoring of depolarization-induced exocytosis from adrenal medullary chromaffin cells and pancreatic islet B cells using "perforated patch recording". Ann N Y Acad Sci 635:464–467
27. Hagiwara S, Byerly L (1981) Calcium channel. Annu Rev Neurosci 4:69–125
28. Hagiwara S, Nakajima S (1966) Effects of the intracellular Ca ion concentration upon the excitability of the muscle fiber membrane of a barnacle. J Gen Physiol 49:807–818
29. Hamill OP, Marty A, Neher E, Sakmann B, Sigworth FJ (1981) Improved patch-clamp techniques for high-resolution current recording from cells and cell-free membrane patches. Pflugers Arch 391:85–100
30. Hernández-Guijo JM, Carabelli V, Gandía L, García AG, Carbone E (1999) Voltage-independent autocrine modulation of L-type channels mediated by ATP, opioids and catecholamines in rat chromaffin cells. Eur J Neurosci 11:3574–3584
31. Hernández-Guijo JM, Gandía L, de Pascual R, García AG (1997) Differential effects of the neuroprotectant lubeluzole on bovine and mouse chromaffin cell calcium channel subtypes. Br J Pharmacol 122:275–285
32. Hernández-Guijo JM, Maneu-Flores VE, Ruiz-Nuno A, Villarroya M, García AG, Gandía L (2001) Calcium-dependent inhibition of L, N, and P/Q Ca^{2+} channels in chromaffin cells: role of mitochondria. J Neurosci 21:2553–2560
33. Jiménez RR, López MG, Sancho C, Maroto R, García AG (1993) A component of the catecholamine secretory response in the bovine adrenal gland is resistant to dihydropyridines and omega-conotoxin. Biochem Biophys Res Commun 191:1278–1283
34. Korn SJ, Horn R (1989) Influence of sodium-calcium exchange on calcium current rundown and the duration of calcium-dependent chloride currents in pituitary cells, studied with whole cell and perforated patch recording. J Gen Physiol 94:789–812
35. Kunze DL, Rampe D (1992) Characterization of the effects of a new Ca^{2+} channel activator, FPL 64176, in GH3 cells. Mol Pharmacol 42:666–670
36. Lara B, Gandía L, Martinez-Sierra R, Torres A, García AG (1998) Q-type Ca^{2+} channels are located closer to secretory sites than L-type channels: functional evidence in chromaffin cells. Pflugers Arch 435:472–478
37. Liang H, DeMaria CD, Erickson MG, Mori MX, Alseikhan BA, Yue DT (2003) Unified mechanisms of Ca^{2+} regulation across the Ca^{2+} channel family. Neuron 39:951–960
38. Liu L, Rittenhouse AR (2003) Arachidonic acid mediates muscarinic inhibition and enhancement of N-type Ca^{2+} current in sympathetic neurons. Proc Natl Acad Sci U S A 100:295–300
39. Livett BG (1984) Adrenal medullary chromaffin cells in vitro. Physiol Rev 64:1103–1161
40. López MG, Villarroya M, Lara B, Martínez-Sierra R, Albillos A, García AG, Gandía L (1994) Q- and L-type Ca^{2+} channels dominate the control of secretion in bovine chromaffin cells. FEBS Lett 349:331–337
41. Lukyanetz EA, Neher E (1999) Different types of calcium channels and secretion from bovine chromaffin cells. Eur J Neurosci 11:2865–2873
42. McDonough SI, Mori Y, Bean BP (2005) FPL 64176 modification of Ca(V) 1.2 L-type calcium channels: dissociation of effects on ionic current and gating current. Biophys J 88:211–223
43. McGuigan JA, Luthi D, Buri A (1991) Calcium buffer solutions and how to make them: a do it yourself guide. Can J Physiol Pharmacol 69:1733–1749
44. McKechnie K, Killingback P, Naya I, O'Conner SE, Smith G, Warfam DG, Wells E, Whitehead YM, Williams G (1989) Calcium channel activator properties in a novel non-dihydropyridine-FPL64176. Br J Pharmacol 98:673–679
45. Monck JR, Robinson IM, Escobar AL, Vergara JL, Fernandez JM (1994) Pulsed laser imaging of rapid Ca^{2+} gradients in excitable cells. Biophys J 67:505–514
46. Montero M, Alonso MT, Albillos A, Cuchillo-Ibáñez I, Olivares R, García AG, García-Sancho J, Alvarez J (2001) Control of secretion by mitochondria depends on the size of the local $[Ca^{2+}]$ after chromaffin cell stimulation. Eur J Neurosci 13:2247–2254
47. Montero M, Alonso MT, Carnicero E, Cuchillo-Ibáñez I, Albillos A, García AG, García-Sancho J, Alvarez J (2000) Chromaffin-cell stimulation triggers fast millimolar mitochondrial Ca^{2+} transients that modulate secretion. Nat Cell Biol 2:57–61
48. Montiel C, Mendoza I, García CJ, Awad Y, García-Olivares J, Solís-Garrido LM, Lara H, García AG, Cárdenas AM (2003) Distinct protein kinases regulate SNAP-25 expression in chromaffin cells. J Neurosci Res 71:353–364
49. Morad M, Soldatov N (2005) Calcium channel inactivation: possible role in signal transduction and Ca^{2+} signaling. Cell Calcium 38:223–231
50. Moro MA, López MG, Gandía L, Michelena P, García AG (1990) Separation and culture of living adrenaline- and noradrenaline-containing cells from bovine adrenal medullae. Anal Biochem 185:243–248
51. Naraghi M, Muller TH, Neher E (1998) Two-dimensional determination of the cellular Ca^{2+} binding in bovine chromaffin cells. Biophys J 75:1635–1647
52. Neely A, Lingle CJ (1992) Two components of calcium-activated potassium current in rat adrenal chromaffin cells. J Physiol 453:97–131
53. Neher E (1998) Usefulness and limitations of linear approximations to the understanding of Ca^{++} signals. Cell Calcium 24:345–357
54. Neher E (1998) Vesicle pools and Ca^{2+} microdomains: new tools for understanding their roles in neurotransmitter release. Neuron 20:389–399
55. Neher E, Augustine GJ (1992) Calcium gradients and buffers in bovine chromaffin cells. J Physiol 450:273–301
56. Nowicky AV, Duchen MR (1998) Changes in $[Ca^{2+}]_i$ and membrane currents during impaired mitochondrial metabolism in dissociated rat hippocampal neurons. J Physiol 507:131–145
57. Nowycky MC, Fox AP, Tsien RW (1985) Three types of neuronal calcium channel with different calcium agonist sensitivity. Nature 316:440–443
58. O'Farrell M, Marley PD (2000) Differential control of tyrosine hydroxylase activation and catecholamine secretion by voltage-operated Ca^{2+} channels in bovine chromaffin cells. J Neurochem 74:1271–1278
59. Olivera BM, Miljanich GP, Ramachandran J, Adams ME (1994) Calcium channel diversity and neurotransmitter release: the omega-conotoxins and omega-agatoxins. Annu Rev Biochem 63:823–867

60. Perissinotti PP, Giugovaz Tropper B, Uchitel OD (2008) L-type calcium channels are involved in fast endocytosis at the mouse neuromuscular junction. Eur J Neurosci 27:1333–1344
61. Rae J, Cooper K, Gates P, Watsky M (1991) Low access resistance perforated patch recordings using amphotericin B. J Neurosci Methods 37:15–26
62. Robinson IM, Finnegan JM, Monck JR, Wightman RM, Fernandez JM (1995) Colocalization of calcium entry and exocytotic release sites in adrenal chromaffin cells. Proc Natl Acad Sci U S A 92:2474–2478
63. Rosa JM, de Diego AM, Gandía L, García AG (2007) L-type calcium channels are preferentially coupled to endocytosis in bovine chromaffin cells. Biochem Biophys Res Commun 357:834–839
64. Sala F, Hernández-Cruz A (1990) Calcium diffusion modeling in a spherical neuron. Relevance of buffering properties. Biophys J 57:313–324
65. Schramm M, Thomas G, Towart R, Franckowiak G (1983) Novel dihydropyridines with positive inotropic action through activation of $Ca2^{+}$ channels. Nature 303:535–537
66. Schroeder TJ, Jankowski JA, Senyshyn J, Holz RW, Wightman RM (1994) Zones of exocytotic release on bovine adrenal medullary cells in culture. J Biol Chem 269:17215–17220
67. Simon SM, Llinas RR (1985) Compartmentalization of the submembrane calcium activity during calcium influx and its significance in transmitter release. Biophys J 48:485–498
68. Tillotson D (1979) Inactivation of Ca conductance dependent on entry of Ca ions in molluscan neurons. Proc Natl Acad Sci U S A 76:1497–1500
69. Ulate G, Scott SR, Gonzalez J, Gilabert JA, Artalejo AR (2000) Extracellular ATP regulates exocytosis in inhibiting multiple Ca^{2+} channel types in bovine chromaffin cells. Pflugers Arch 439:304–314
70. Villarroya M, Olivares R, Ruiz A, Cano-Abad MF, de Pascual R, Lomax RB, Lopez MG, Mayorgas I, Gandia L, Garcia AG (1999) Voltage inactivation of Ca^{2+} entry and secretion associated with N- and P/Q-type but not L-type Ca^{2+} channels of bovine chromaffin cells. J Physiol 516:421–432
71. von Gersdorff H, Matthews G (1996) Calcium-dependent inactivation of calcium current in synaptic terminals of retinal bipolar neurons. J Neurosci 16:115–122
72. von Ruden L, Garcia AG, Lopez MG (1993) The mechanism of Ba^{2+}-induced exocytosis from single chromaffin cells. FEBS Lett 336:48–52
73. Wick PF, Trenkle JM, Holz RW (1997) Punctate appearance of dopamine-beta-hydroxylase on the chromaffin cell surface reflects the fusion of individual chromaffin granules upon exocytosis. Neuroscience 80:847–860
74. Xu T, Naraghi M, Kang H, Neher E (1997) Kinetic studies of Ca^{2+} binding and Ca^{2+} clearance in the cytosol of adrenal chromaffin cells. Biophys J 73:532–545
75. Zheng W, Rampe D, Triggle DJ (1991) Pharmacological, radioligand binding, and electrophysiological characteristics of FPL 64176, a novel nondihydropyridine Ca^{2+} channel activator, in cardiac and vascular preparations. Mol Pharmacol 40:734–741
76. Zhou Z, Neher E (1993) Mobile and immobile calcium buffers in bovine adrenal chromaffin cells. J Physiol 469:245–273